



Research Article

Cancel-Decode-Encode Processing on Two-Way Cooperative NOMA Schemes in Realistic Conditions

Thu-Thuy Thi Dao ^{1,2} and Pham Ngoc Son ¹

¹Ho Chi Minh City University of Technology and Education, Ho Chi Minh City, Vietnam

²Industrial University of Ho Chi Minh City, Ho Chi Minh City, Vietnam

Correspondence should be addressed to Thu-Thuy Thi Dao; thuydt.ncs@hcmute.edu.vn and Pham Ngoc Son; sonpndtvt@hcmute.edu.vn

Received 28 July 2020; Revised 1 March 2021; Accepted 22 March 2021; Published 28 April 2021

Academic Editor: Alessandro Bazzi

Copyright © 2021 Thu-Thuy Thi Dao and Pham Ngoc Son. This is an open access article distributed under the Creative Commons Attribution License, which permits unrestricted use, distribution, and reproduction in any medium, provided the original work is properly cited.

This paper considers the effects of perfect/imperfect successive interference cancellation (SIC) and perfect/imperfect information (CSI) in a multiple-relay two-way cooperative network using nonorthogonal multiple access (NOMA) and digital network coding (DNC). In this model, a relay is selected by maximizing estimated channel gains to enhance the decoding capacity of the nearer source and minimize the collection time of imperfect CSI. Spectrum utilization efficiency is enhanced two times by a mixture of the SIC and DNC techniques at the selected relay (called as the SIC-2TS protocol). The system performance is considered through analysis of the exact and asymptotic expressions of the system outage probabilities and throughput. The major thing is exposed as the proposed SIC-2TS protocol can reach the best performance at optimal positions of the selected relay. Besides, the system throughput of the proposed protocol outperforms a SIC-utilized two-way relaying scheme without the DNC (called as the SIC-3TS protocol) and a conventional two-way scheme (called as the CONV-4TS protocol) for all signal-to-noise ratio regions. Lastly, the validity of the analytical expressions is verified by the Monte Carlo simulation results.

1. Introduction

Recently, wireless networks have rising challenges in enhancing system throughput and spectrum efficiency owing to the increasing user devices and increasing various Internet of Things applications. A key technology for the fifth-generation wireless network to solve these challenges is NOMA technology because of its attainments to help grow spectral efficiency, enlarge connections, decrease access latency, and increase the users' fairness [1–3]. Power domain NOMA uses the superposition coding to allocate different power levels for transmitted signals to the multiusers at the same time, frequency, and code domains. At receivers, the successive interference cancellation method is applied to decode the received signals [2, 3]. However, unexpected errors in decoding when using SIC still occur due to the complexity scale and error propagation, leading to the near user enduring a residual interference signal and the NOMA system performance impacted by this imperfect SIC (ipSIC) [3–6]. In [7],

the authors investigated the reliability and security of the ambient backscatter NOMA systems, where the source was aimed at communicating with two NOMA users in the presence of an eavesdropper. The authors in [7] considered a more practical case that nodes and backscatter devices suffer from in-phase and quadrature-phase imbalance.

Besides, cooperative communication has also been widely studied because its spatial diversity advantage helps to reduce fading, widen coverage, and increase communication preciseness [6, 8–10]. In conventional cooperative communications, relaying nodes apply the decode-and-forward (DF) method or the amplify-and-forward (AF) method to process their received and transmitted signals [6, 11]. The DF method is better because it decodes received signals at the relay, then reencodes them for forwarding to the destination so it does not amplify noises in received signals like the AF.

Cooperative models show that the selection of the best-relaying devices, including partial relay selection and opportunistic relay selection, is necessary to improve system

performance [5, 11–19]. These methods are based on the collection of channel state information to select the optimal relay to support communication. The partial relay selection does not offer the full spatial diversity, but it is not as complicated as the full relay selection, and it is useful for applications in industrial IoT and wireless sensor networks. In most practical applications, CSIs cannot be perfectly measured and there are some mismatch, known as imperfect CSIs (ipCSIs) [12, 14, 16, 19–22]. The mismatch can happen due to the feedback delays of the CSIs [12, 14, 16, 19, 22] or the faults in the CSI estimating process [20, 21]. One-way NOMA and cooperative NOMA (CNOMA) networks with the SIC have been widely discussed to increase spectral efficiency gain, improve secure performance, enlarge system energy efficiency, and enhance significantly sum throughput in several studies [1, 4, 23–25]. Besides, two-way cooperative networks have advantages in using frequency spectral efficiency over one-way networks because two sources are able to both transmit and receive signals. Moreover, network coding has the advantages of compressing data and high spectral efficiency, and it plays a crucial role in two-way relay networks [5].

In this paper, we propose a two-way cooperative network with a cluster of DF relays and two sources in which the relay will be chosen in the setup phase. The relay selection method in our work helps to enhance the decoding capacity of the nearer source and decrease the collection time of the CSIs than the opportunistic relay selection in [5]. To achieve higher spectral efficiency, we use the NOMA protocol for uplink and the DNC technique for downlink. At the selected relay, the SIC is used to decode sequentially the received signals; next, the DNC is applied to create a new encoded signal and then, this signal is transmitted back to sources, called as the SIC-2TS protocol. Moreover, this paper also investigates the effect of realistic conditions as the ipCSIs and the ipSIC on the system performance. Afterward, the system performance of the SIC-2TS protocol is evaluated based on the analysis expressions of the outage probabilities and the system throughput. Lastly, we compare the proposed protocol with the conventional two-way DF protocol, denoted as CONV-4TS protocol, and the SIC-utilized two-way relaying without the DNC, denoted as the SIC-3TS protocol.

The contributions in this paper are summarized as follows. Firstly, the exact and asymptotic expressions of the outage probabilities and throughput of two sources in the proposed scheme are analyzed and verified under the overall effects of pSIC/ipSIC and pCSIs/ipCSI conditions. Secondly, the exact and asymptotic closed-form expressions are proved valid by the simulation results. Next, the simulation results show that the ipSIC and the ipCSI conditions significantly affect the system performance. Fourthly, the performance of the SIC-2TS protocol is improved by the increased number of relays as well as the perfect operations of the SIC process and the CSI estimations. Moreover, the performance of SIC-2TS can attain the best level at optimal locations of the selected relay and the power suitable coefficients of two sources. Last but not the least, the system throughput of the proposed method outperforms the conventional CONV-

TABLE 1: Notation table.

Notation	Meaning
N	Number of relays
$f_X(\cdot)$	Probability density function (PDF) of X
$F_X(\cdot)$	Cumulative distribution function (CDF) of X
\oplus	XOR operation
$\max(\cdot)$	Find the maximum value
$\operatorname{argmax}(\cdot)$	Find an element to achieve the maximum value
α_k	Power allocation coefficient of the source S_k
$\Pr(\cdot)$	Probability operation
γ_t	Target signal-to-interference-plus-noise ratio (SINR)
OP_{S_k}	Outage probability at the source S_k
TP	Throughput (bits/s/Hz)

4TS and SIC-3TS protocols in both cases of pCSIs and ipCSIs for all SNR regions.

The rest of our paper is organized as follows. Section 2 shows some related works. Section 3 describes the system model. Section 4 analyzes the system performance of the SIC-2TS, SIC-3TS, and CONV-4TS protocols. Section 5 shows the results and respective discussions. Finally, section 6 summarizes contributions in this paper.

Notations used in this paper are listed in Table 1.

2. Related Works

In recent researches, specific two-way CNOMA (TWR CNOMA) networks have been investigated to take benefit on system performance. The performance of the NOMA-based two-way relaying network for uplink and downlink of two users or two groups in the perfect SIC (pSIC) and ipSIC conditions and Rayleigh fading was analyzed with a half-duplex DF relay in [26, 27] and a full-duplex DF relay in [28]. The works in [26–28] showed that two-way NOMA is superior to two-way orthogonal multiple access (OMA) in terms of outage probability in low signal-to-noise ratio (SNR) regimes. In [29], the joint effects of in-phase and quadrature-phase imbalance and ipSIC on the performance of TWR CNOMA networks over the Rician fading channels were studied. Besides, the realistic assumptions of the residual hardware impairments or ipCSIs of two-way or multiway CNOMA networks have also been considered in the articles [21, 22, 30].

Moreover, DNC and NOMA techniques can be combined to decreasing transmission time between devices and improve the performance system [5, 31, 32]. In [31, 32], the authors combined NOMA and DNC techniques in a two-way DF relay cooperative scheme confirming that performance in this proposed asymmetric scheme had better spectrum utilization efficiency than the traditional two-way DF OMA scheme, the two-way DF with only using the CNOMA, and the two-way relaying system with OMA in the uplink and DNC in the downlink. The authors in [31, 32] only used

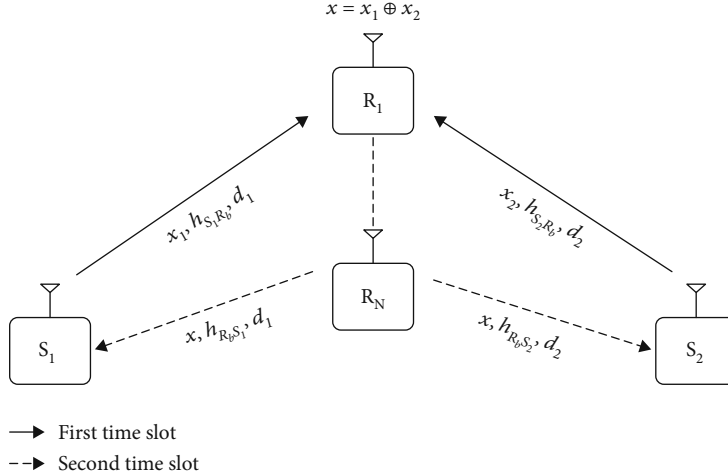


FIGURE 1: Two-way cooperative model of the SIC-2TS protocol.

a DF relay to support communication. The system performance in [31] was considered in the case of the ideal conditions. In [5], the system performance was investigated in perfect CSI (pCSI) conditions with the opportunistic relay selection.

3. System Model

A cooperative two-way network has two sources S_1 and S_2 and a closed group of N half-duplex DF relays R_i with $i \in \{1, 2, \dots, N\}$, as depicted in Figure 1. This system model can be applied for data transmission in heterogeneous cellular networks. The sources and the relays in the SIC-2TS are single antenna and HD devices. We assume that the direct link between the two sources does not exist due to severe fading and path loss, and the information exchange can be performed only via relays [32–34]; the relays are close together as a cluster [17] so the link distances between each source and the relays are identical; hence, we denote d_1 and d_2 as the normalized distances between S_1 and R_i and between S_2 and R_i , respectively. We also assume that the flat and block Rayleigh fading channels with the fading coefficients for links $S_k \rightarrow R_i$ and $R_i \rightarrow S_k$ are denoted as $h_{S_k R_i}$ and $h_{R_i S_k}$, respectively, where $k \in \{1, 2\}$. In addition, perfect knowledge of all links is assumed at the receivers by channel estimators that are error-free [35], and the ipCSIs are only caused by the feedback delay with a time-variant channel representation and is described by [12, 14, 16, 20, 22, 32, 35]

$$\hat{h}_v = \rho_v h_v + \sqrt{1 - \rho_v^2} \varepsilon_v, \quad (1)$$

where $v \in \{S_k R_i, R_i S_k\}$. Here, ε_v stand for the estimation errors and \hat{h}_v describes the estimated CSIs. ε_v and \hat{h}_v are independent complex Gaussian random variables (RVs) with zero means and variances λ_v , ($\varepsilon_v, \hat{h}_v \sim CN(0, \lambda_v)$) [14, 16].

And the correlation coefficients ρ_v ($0 \leq \rho_v \leq 1$) are constants (where $\rho_v = 1$ denotes no delay effect), characterizing the average quality of channel estimations [14, 16, 32]. For uncomplicated, we assume that $\rho_v = \rho$ for all the similar devices, $\rho = 1$ for perfect CSIs, and $\rho < 1$ for ipCSIs [12, 14, 16, 20, 32]. The estimated channel gains $g_{S_k R_i} = |\hat{h}_{S_k R_i}|^2$ and $g_{R_i S_k} = |\hat{h}_{R_i S_k}|^2$ are exponentially distributed RVs with PDFs $f_{g_{S_k R_i}}(x) = f_{g_{R_i S_k}}(x) = (1/\lambda_k) e^{-x/\lambda_k}$, and CDFs $F_{g_{S_k R_i}}(x) = F_{g_{R_i S_k}}(x) = 1 - e^{-x/\lambda_k}$, where $\lambda_k = \lambda_{S_k R_i} = \lambda_{R_i S_k} = d_k^{-\beta}$ and β is a path-loss exponent [15].

Prior to transmitting data, the setup phase is performed firstly by request and feedback messages through the cooperative medium access control (MAC) protocol [8]. The nearer source, denoted as S_n , $n \in \{1, 2\}$, receives all channel coefficients from it to the relays under effect of feedback delay and performs the cooperative relay selection. The SIC-2TS protocol uses two time slots for signal communication. In the first slot, two sources S_1 and S_2 send concurrently their signals x_1 and x_2 , respectively, to all relays, and at the selected relay, the SIC technique is applied to decode the received signals. In the second slot, the DNC technique is used to create a new signal $x = x_1 \oplus x_2$ [5, 15, 32] and the selected relay sends it back to two sources S_1 and S_2 with transmit power P_R .

The signal which the relays receive in the first time slot is a weighted sum of x_1 and x_2 as follows:

$$y_{R_i} = \sqrt{\alpha_1 P_S} h_{S_1 R_i} x_1 + \sqrt{\alpha_2 P_S} h_{S_2 R_i} x_2 + n_{R_i}, \quad (2)$$

where $\alpha_1 P_S$ and $\alpha_2 P_S$ are transmit powers to carry x_1 and x_2 , respectively; α_1 and α_2 are power allocation coefficients to fairness between two sources (a lower power should be given to the source which is nearer relays) [28], ($0 < \alpha_1, \alpha_2 < 1$); and n_{R_i} is the AWGNs with the variance N_0 at the nodes R_i .

Substituting (1) into (2), the received signal is given by

$$\begin{aligned}
y_{R_i} &= \sqrt{\alpha_1 P_S} \left(\frac{\hat{h}_{S_1 R_i} - \sqrt{1-\rho^2} \varepsilon_{S_1 R_i}}{\rho} \right) x_1 \\
&\quad + \sqrt{\alpha_2 P_S} \left(\frac{\hat{h}_{S_2 R_i} - \sqrt{1-\rho^2} \varepsilon_{S_2 R_i}}{\rho} \right) x_2 + n_{R_i} \\
&= \sqrt{\alpha_1 P_S} \hat{h}_{S_1 R_i} x_1 + \sqrt{\alpha_2 P_S} \hat{h}_{S_2 R_i} x_2 \\
&\quad - \sqrt{\alpha_1 P_S} \frac{\sqrt{1-\rho^2}}{\rho} \varepsilon_{S_1 R_i} x_1 \\
&\quad - \sqrt{\alpha_2 P_S} \frac{\sqrt{1-\rho^2}}{\rho} \varepsilon_{S_2 R_i} x_2 + n_{R_i}.
\end{aligned} \tag{3}$$

Due to the symmetry of the proposed system model in Figure 1, without loss of generality, assume that S_n and S_f are near and far sources from the relays, respectively, where $n, f \in \{1, 2\}$ and $n \neq f$. Applying the SIC technique [5, 6, 24, 27, 32], firstly, the relays decode the signal x_n of the nearby source which has better average channel quality while the signal x_f is considered as interference. The received signal-to-interference-plus-noise ratio (SINR) for detecting x_n is given by

$$\begin{aligned}
\gamma_{S_n R_i \rightarrow x_n | d_n \leq d_f} &= \frac{\alpha_n P_S \left| \hat{h}_{S_n R_i} \right|^2 / \rho^2}{\alpha_f P_S \left| \hat{h}_{S_f R_i} \right|^2 / \rho^2 + (\alpha_n P_S \lambda_{S_n R_i} + \alpha_f P_S \lambda_{S_f R_i}) (1-\rho^2) / \rho^2 + N_0} \\
&= \frac{\alpha_n \gamma \left| \hat{h}_{S_n R_i} \right|^2}{\alpha_f \gamma \left| \hat{h}_{S_f R_i} \right|^2 + \gamma (\alpha_n \lambda_n + \alpha_f \lambda_f) (1-\rho^2) + \rho^2} \\
&= \frac{\alpha_n \left| \hat{h}_{S_n R_i} \right|^2}{\alpha_f \left| \hat{h}_{S_f R_i} \right|^2 + \underbrace{(\alpha_n \lambda_n + \alpha_f \lambda_f) (1-\rho^2) + \rho^2}_{\phi_1} / \gamma} \\
&= \frac{\alpha_n g_{S_n R_i}}{\alpha_f g_{S_f R_i} + \phi_1},
\end{aligned} \tag{4}$$

where γ is the transmit SNR, $\gamma = P_S / N_0$.

In this paper, the relay selection method is used by maximizing estimated channel gains to enhance the decoding capacity of the nearer source. This method has an outstanding advantage in minimizing the collection time of ipCSIs. The relay selection criterion based on the estimated channel gains has been used in [36–38] to achieve the better performance. From (4), the selected relay R_b is expressed as follows:

$$R_b = \arg \max_{i=1 \dots N} g_{S_n R_i}. \tag{5}$$

After decoding x_n successfully, the relay R_b deletes the component containing the x_n signal in (3); then, it decodes

the x_f signal and the received SINR for detecting x_f is given by

$$\begin{aligned}
\gamma_{S_f R_b \rightarrow x_f | d_n \leq d_f} &= \frac{\alpha_f P_S \left| \hat{h}_{S_f R_b} \right|^2 / \rho^2}{\varepsilon P_S \left| h_{R_b} \right|^2 + (\alpha_n P_S \lambda_n + \alpha_f P_S \lambda_f) (1-\rho^2) / \rho^2 + N_0} \\
&= \frac{\alpha_f \gamma \left| \hat{h}_{S_f R_b} \right|^2}{\varepsilon \gamma \left| h_{R_b} \right|^2 + \gamma (\alpha_n \lambda_n + \alpha_f \lambda_f) (1-\rho^2) + \rho^2} \\
&= \frac{\alpha_f g_{S_f R_b}}{\varepsilon \rho^2 g_{R_b} + \phi_1},
\end{aligned} \tag{6}$$

where h_{R_b} is a remaining interference signal with zero mean and variance Ω at the relay R_b [27], $g_{R_b} = |h_{R_b}|^2$ is exponentially distributed RVs with the PDF as $f_{g_{R_b}}(x) = (1/\Omega)e^{-x/\Omega}$, and CDF $F_{g_{R_b}}(x) = 1 - e^{-x/\Omega}$ [27, 28]. $\varepsilon = 0$ and $\varepsilon = 1$ correspond to ipSIC and ipSIC at the relay R_b , respectively [5, 28].

In the second time slot, at the relay R_b , the signal $x = x_1 \oplus x_2$ is synthesized and transmitted to two sources. And the received signal at the source S_k , $k \in \{1, 2\}$, is described as follows:

$$\begin{aligned}
y_{R_b S_k} &= \sqrt{P_R} h_{R_b S_k} x + n_{S_k} \\
&= \sqrt{P_R} \hat{h}_{R_b S_k} x - \sqrt{P_R} \frac{\sqrt{1-\rho^2}}{\rho} \varepsilon_{R_b S_k} x + n_{S_k},
\end{aligned} \tag{7}$$

where n_{S_k} is the AWGNs at the sources S_k with the variance N_0 .

Next, the x signal is detected at the two sources with the SINR as follows:

$$\gamma_{R_b S_k \rightarrow x} = \frac{P_R \left| \hat{h}_{R_b S_k} \right|^2 / \rho^2}{P_R \lambda_k (1-\rho^2) / \rho^2 + N_0} = \frac{\eta \gamma g_{R_b S_k}}{\eta \gamma \lambda_k (1-\rho^2) + \rho^2}, \tag{8}$$

where $\eta = P_R / P_S$ and $\eta > 0$.

Remark 1. If the proposed SIC-2TS protocol operates without the DNC at the selected relay, the signals x_1 and x_2 are sent sequences by the R_b to the sources S_2 and S_1 in two different time slots (the second and third time slots). The received signals and the corresponding SINRs are expressed identically as formulas (7) and (8) in which the symbol x is changed to x_1 (to send S_2) and x_2 (to send S_1). We denoted the SIC-2TS protocol in this case (without the DNC) as the SIC-3TS protocol to distinguish in the rest of this paper.

We also investigate a conventional two-way CONV-4TS protocol using four time slots with relay selection. This protocol's transmission process is as follows: $S_1 \xrightarrow[1st]{x_1} R_{b1} \xrightarrow[2nd]{x_1} S_2$
 $\xrightarrow[3rd]{x_2} R_{b2} \xrightarrow[4th]{x_2} S_1$.

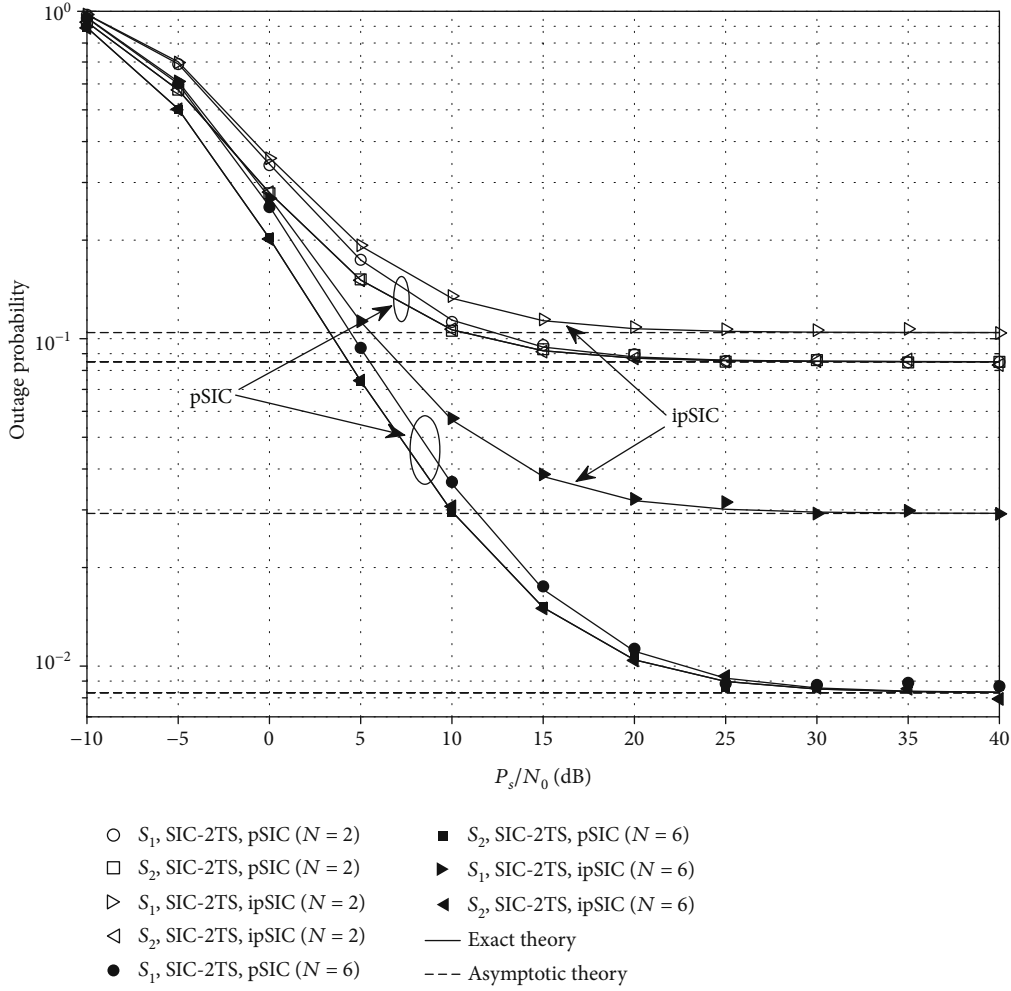


FIGURE 2: Outage probabilities of the source nodes S_1 and S_2 in the proposed SIC-2TS protocol versus P_S/N_0 (dB) when $\Omega = -10$ (dB), $d_1 = 0.4$, $d_2 = 1 - d_1$, $N \in \{2, 6\}$, $\rho \in \{0.92, 1\}$, $\varepsilon = 0$, and the power allocation coefficients $\alpha_1 = \alpha_2 = \eta = 1$.

Firstly, the data signal x_1 is transmitted from the source S_1 to all the relays; the received signal and the SINR at the relay R_i are described by

$$\begin{aligned} y_{S_1 R_i}^C &= \sqrt{\alpha_1 P_S} h_{S_1 R_i} x_1 + n_{R_i} \\ &= \sqrt{\alpha_1 P_S} \left(\frac{\hat{h}_{S_1 R_i} - \sqrt{1 - \rho^2} \varepsilon_{S_1 R_i}}{\rho} \right) x_1 + n_{R_i} \\ &= \sqrt{\alpha_1 P_S} \hat{h}_{S_1 R_i} x_1 - \sqrt{\alpha_1 P_S} \frac{\sqrt{1 - \rho^2}}{\rho} \varepsilon_{S_1 R_i} x_1 + n_{R_i}, \end{aligned} \quad (9)$$

$$\gamma_{S_1 R_i} = \frac{\alpha_1 P_S |\hat{h}_{S_1 R_i}|^2 / \rho^2}{\alpha_1 P_S \lambda_1 (1 - \rho^2) / \rho^2 + N_0} = \frac{\alpha_1 \gamma g_{S_1 R_i}}{\alpha_1 \lambda_1 \gamma (1 - \rho^2) + \rho^2}. \quad (10)$$

Secondly, the relay R_{b_1} is selected as by formula $R_{b_1} = \arg \max_{i=1 \dots N} g_{S_1 R_i}$ and then R_{b_1} decodes and transmits the signal

x_1 to the source S_2 . The received signal and the SINR at the source S_2 are described by

$$\begin{aligned} y_{R_{b_1} S_2}^C &= \sqrt{P_R} \hat{h}_{R_{b_1} S_2} x_1 + n_{S_2} \\ &= \sqrt{P_R} \hat{h}_{R_{b_1} S_2} x_1 - \sqrt{P_R} \frac{\sqrt{1 - \rho^2}}{\rho} \varepsilon_{R_{b_1} S_2} x_1 + n_{S_2}, \end{aligned} \quad (11)$$

$$\gamma_{R_{b_1} S_2} = \frac{P_R |\hat{h}_{R_{b_1} S_2}|^2 / \rho^2}{P_R \lambda_2 (1 - \rho^2) / \rho^2 + N_0} = \frac{\eta \gamma g_{R_{b_1} S_2}}{\eta \gamma \lambda_2 (1 - \rho^2) + \rho^2}. \quad (12)$$

In the same way, in the third and fourth time slots, the source S_2 transmits the signal x_2 to the source S_1 via the best relay R_{b_2} . We have the SINRs to decode the signal x_2 at the relay R_i and the source S_1 as follows:

$$\gamma_{S_2 R_i} = \frac{\alpha_f P_S \left| \hat{h}_{S_2 R_i} \right|^2 / \rho^2}{\alpha_2 P_S \lambda_2 (1 - \rho^2) / \rho^2 + N_0} = \frac{\alpha_2 \gamma \mathcal{G}_{S_2 R_i}}{\alpha_2 \lambda_2 \gamma (1 - \rho^2) + \rho^2}, \quad (13)$$

$$\gamma_{R_b S_1} = \frac{P_R \left| \hat{h}_{R_b S_1} \right|^2 / \rho^2}{P_R \lambda_1 (1 - \rho^2) / \rho^2 + N_0} = \frac{\eta \gamma \mathcal{G}_{R_b S_1}}{\eta \gamma \lambda_1 (1 - \rho^2) + \rho^2}. \quad (14)$$

4. Performance Analysis

Section IV presents expressions of the outage probability and throughput for the protocols. We assume that the outage occurs at the nodes R_i and S_k if their SINRs are less than a predefined target γ_t . Conversely, these nodes decode signals successfully.

4.1. Outage Probability Analysis

4.1.1. The Proposed SIC-2TS Protocol

(1) *The Outage Probability at the Source S_f for the $S_n \rightarrow^{x_n} R_b \rightarrow^x S_f$ Link.* The outage of the system occurs in this link when the relay R_b fails to decode the signal x_n or it decodes successfully the signal x_n but the source S_f fails to decode the signal x . Besides, the outage probability can also be calculated by the complementary event of the success transmission probability. The successful transmission is the signal x_n , and the signal x is received and decoded successfully at the R_b and the source S_f , respectively [32]. At the source S_f , the outage probability of the signal x_n can be described as

$$\begin{aligned} \text{OP}_{S_f} \Big|_{d_n \leq d_f} &= \Pr \left[\gamma_{S_n R_b \rightarrow x_n | d_n \leq d_f} < \gamma_t \right] \\ &\quad + \Pr \left[\gamma_{S_n R_b \rightarrow x_n | d_n \leq d_f} \geq \gamma_t, \gamma_{R_b S_f \rightarrow x} < \gamma_t \right] \\ &= 1 - \Pr \left[\gamma_{S_n R_b \rightarrow x_n | d_n \leq d_f} \geq \gamma_t, \gamma_{R_b S_f \rightarrow x} \geq \gamma_t \right]. \end{aligned} \quad (15)$$

A point to remark is that $\gamma_{S_n R_b \rightarrow x_n | d_n \leq d_f} \geq \gamma_t$ and $\gamma_{R_b S_f \rightarrow x} \geq \gamma_t$ are separate events. Thus, the $\text{OP}_{S_f} \Big|_{d_n \leq d_f}$ can be given by

$$\begin{aligned} \text{OP}_{S_f} \Big|_{d_n \leq d_f} &= 1 - \Pr \left[\gamma_{S_n R_b \rightarrow x_n | d_n \leq d_f} \geq \gamma_t \right] \\ &\quad \times \Pr \left[\gamma_{R_b S_f \rightarrow x} \geq \gamma_t \right]. \end{aligned} \quad (16)$$

Lemma 2. *The probability $\Pr \left[\gamma_{S_n R_b \rightarrow x_n | d_n \leq d_f} \geq \gamma_t \right]$ is calculated by*

$$\Pr \left[\gamma_{S_n R_b \rightarrow x_n | d_n \leq d_f} \geq \gamma_t \right] = 1 - \lambda_n \sum_{p=0}^N \frac{C_N^p (-1)^p e^{-p\phi_3 / \lambda_n}}{\lambda_n + p\phi_2 \lambda_f}, \quad (17)$$

where $\phi_2 = \gamma_t \alpha_f / \alpha_n$, $\phi_3 = \gamma_t \phi_1 / \alpha_n$, and $C_N^p = N! / (p!(N-p)!)$.

Proof. See the proof in ‘‘Appendix A.’’

The probability $\Pr \left[\gamma_{R_b S_f \rightarrow x} \geq \gamma_t \right]$ is solved as

$$\begin{aligned} \Pr \left[\gamma_{R_b S_f \rightarrow x} \geq \gamma_t \right] &= 1 - \Pr \left[\gamma_{R_b S_f \rightarrow x} < \gamma_t \right] \\ &= 1 - \Pr \left[g_{R_b S_f} < \gamma_t \lambda_f (1 - \rho^2) + \frac{\gamma_t \rho^2}{\eta \gamma} \right] \\ &= 1 - F_{g_{R_b S_f}} \left(\gamma_t \lambda_f (1 - \rho^2) + \frac{\gamma_t \rho^2}{\eta \gamma} \right) \\ &= e^{-\gamma_t \left((1 - \rho^2) + (\rho^2 / (\lambda_f \eta \gamma)) \right)}. \end{aligned} \quad (18)$$

Substituting (17) and (18) into (16), the outage probability at the source S_f is obtained as

$$\begin{aligned} \text{OP}_{S_f} \Big|_{d_n \leq d_f} &= 1 - \left(1 - \lambda_n \sum_{p=0}^N \frac{C_N^p (-1)^p e^{-p\phi_3 / \lambda_n}}{\lambda_n + p\phi_2 \lambda_f} \right) \\ &\quad \cdot \left(e^{-\gamma_t \left((1 - \rho^2) + (\rho^2 / (\lambda_f \eta \gamma)) \right)} \right). \end{aligned} \quad (19)$$

(2) *The Outage Probability at the Source S_n for the $S_f \rightarrow^{x_f} R_b \rightarrow^x S_n$ Link.* The outage of the system occurs in this link when the signal x_n is not decoded successfully at relay R_b ; or it is decoded successfully but the signal x_f is not decoded successfully at relay R_b ; or both the signals x_n and x_f are decoded successfully at the relay R_b but the source S_n decodes unsuccessfully the signal x . Conversely, the success transmission of the signal x_f occurs when the relay R_b and the source S_n decode successfully the signals (x_n, x_f) and the signal x , respectively. At the source S_n , the outage probability of the signal x_f can be described as

$$\begin{aligned} \text{OP}_{S_n} \Big|_{d_n \leq d_f} &= \Pr \left[\gamma_{S_n R_b \rightarrow x_n | d_n \leq d_f} < \gamma_t \right] \\ &\quad + \Pr \left[\gamma_{S_n R_b \rightarrow x_n | d_n \leq d_f} \geq \gamma_t, \gamma_{S_f R_b \rightarrow x_f | d_n \leq d_f} < \gamma_t \right] \\ &\quad + \Pr \left[\gamma_{S_n R_b \rightarrow x_n | d_n \leq d_f} \geq \gamma_t, \gamma_{S_f R_b \rightarrow x_f | d_n \leq d_f} \geq \gamma_t, \gamma_{R_b S_n \rightarrow x} < \gamma_t \right] \\ &= 1 - \Pr \left[\gamma_{S_n R_b \rightarrow x_n | d_n \leq d_f} > \gamma_t, \gamma_{S_f R_b \rightarrow x_f | d_n \leq d_f} > \gamma_t, \gamma_{R_b S_n \rightarrow x} > \gamma_t \right] \\ &= 1 - \Pr \left[\gamma_{S_n R_b \rightarrow x_n | d_n \leq d_f} \geq \gamma_t, \gamma_{S_f R_b \rightarrow x_f | d_n \leq d_f} \geq \gamma_t \right] \times \Pr \left[\gamma_{R_b S_n \rightarrow x} \geq \gamma_t \right]. \end{aligned} \quad (20)$$

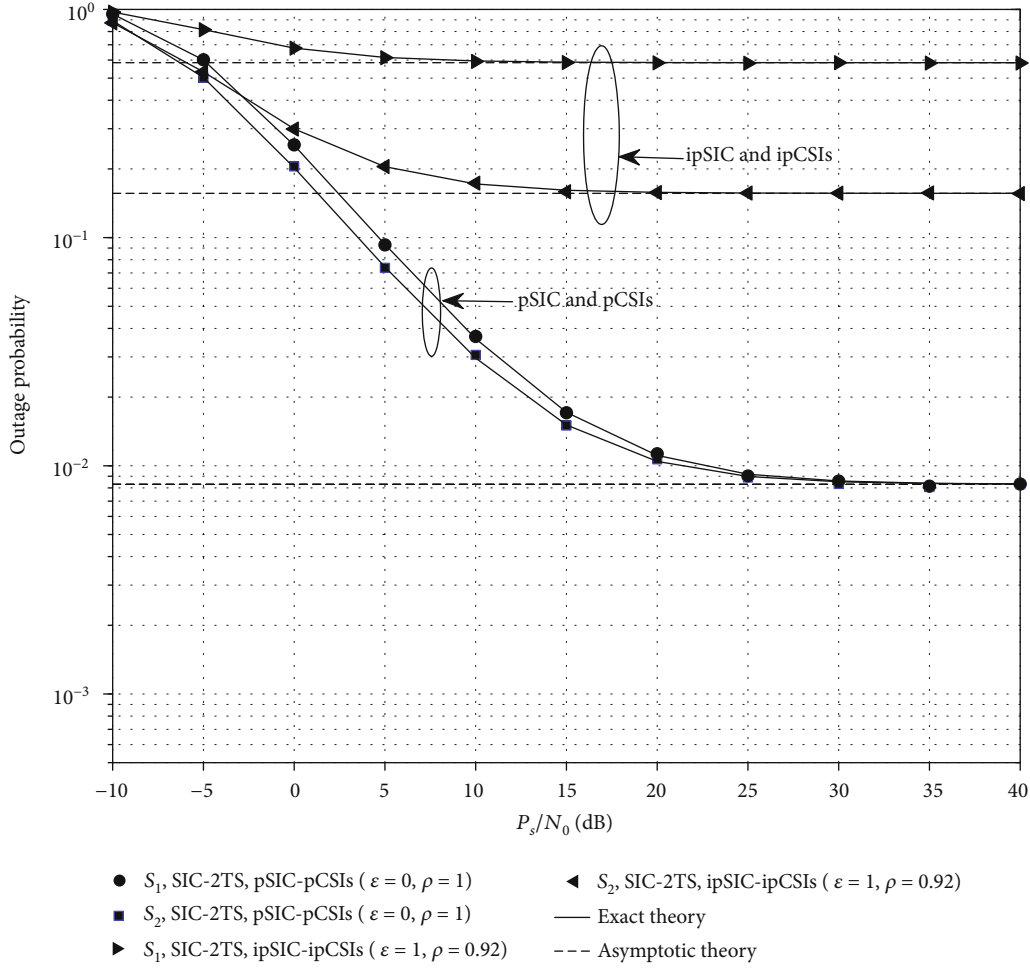


FIGURE 3: Outage probabilities of the source nodes S_1 and S_2 in the proposed SIC-2TS protocol versus P_s/N_0 (dB) when $\Omega = -10$ (dB), $d_1 = 0.4$, $d_2 = 1 - d_1$, $N \in \{2, 6\}$, $\rho = 1$, $\varepsilon \in \{0, 1\}$, and the power allocation coefficients $\alpha_1 = \alpha_2 = \eta = 1$.

Lemma 3. The probability $\Pr[\gamma_{S_n R_b \rightarrow x_n | d_n \leq d_f} \geq \gamma_t, \gamma_{S_f R_b \rightarrow x_f | d_n \leq d_f} \geq \gamma_t]$ is calculated by

$$\Pr\left(\gamma_{S_n R_b \rightarrow x_n | d_n \leq d_f} \geq \gamma_t, \gamma_{S_f R_b \rightarrow x_f | d_n \leq d_f} \geq \gamma_t\right) = \frac{\lambda_f e^{-(\phi_3/\lambda_f)}}{(\lambda_f + \phi_4 \Omega)} - \sum_{p=0}^N \frac{\lambda_n^2 \lambda_f C_N^p (-1)^p e^{-p(\phi_3 + \phi_5 \phi_2)/\lambda_n + \phi_5/\lambda_f}}{(\lambda_n + p\phi_2 \lambda_f)(\lambda_n \lambda_f + \phi_4 \Omega (\lambda_n + p\phi_5 \phi_2 \lambda_f))}, \quad (21)$$

where $\phi_4 = \gamma_t \varepsilon \rho^2 / \alpha_f$ and $\phi_5 = \gamma_t \phi_1 / \alpha_f$.

Proof. See the proof in ‘‘Appendix B.’’

The final probability $\Pr[\gamma_{R_b S_n \rightarrow x} \geq \gamma_t]$ in (20) is answered as

$$\begin{aligned} \Pr[\gamma_{R_b S_n \rightarrow x} \geq \gamma_t] &= 1 - \Pr[\gamma_{R_b S_n \rightarrow x} < \gamma_t] \\ &= 1 - \Pr\left[g_{R_b S_n} < \gamma_t \lambda_n (1 - \rho^2) + \frac{\gamma_t \rho^2}{\eta \gamma}\right] \\ &= e^{-\gamma_t ((1 - \rho^2) + \rho^2 / (\lambda_n \eta \gamma))}. \end{aligned} \quad (22)$$

By substituting (21) and (22) into (20), the outage probability at the source S_n is solved as

$$\text{OP}_{S_n | d_n \leq d_f} = 1 - \left(\frac{\lambda_f e^{-\phi_5/\lambda_f}}{(\lambda_f + \phi_4 \Omega)} - \sum_{p=0}^N \frac{\lambda_n^2 \lambda_f C_N^p (-1)^p e^{-p(\phi_3 + \phi_5 \phi_2)/\lambda_n + \phi_5/\lambda_f}}{(\lambda_n + p\phi_2 \lambda_f)(\lambda_n \lambda_f + \phi_4 \Omega (\lambda_n + p\phi_5 \phi_2 \lambda_f))} \right) \times \left(e^{-\gamma_t ((1 - \rho^2) + \rho^2 / (\lambda_n \eta \gamma))} \right). \quad (23)$$

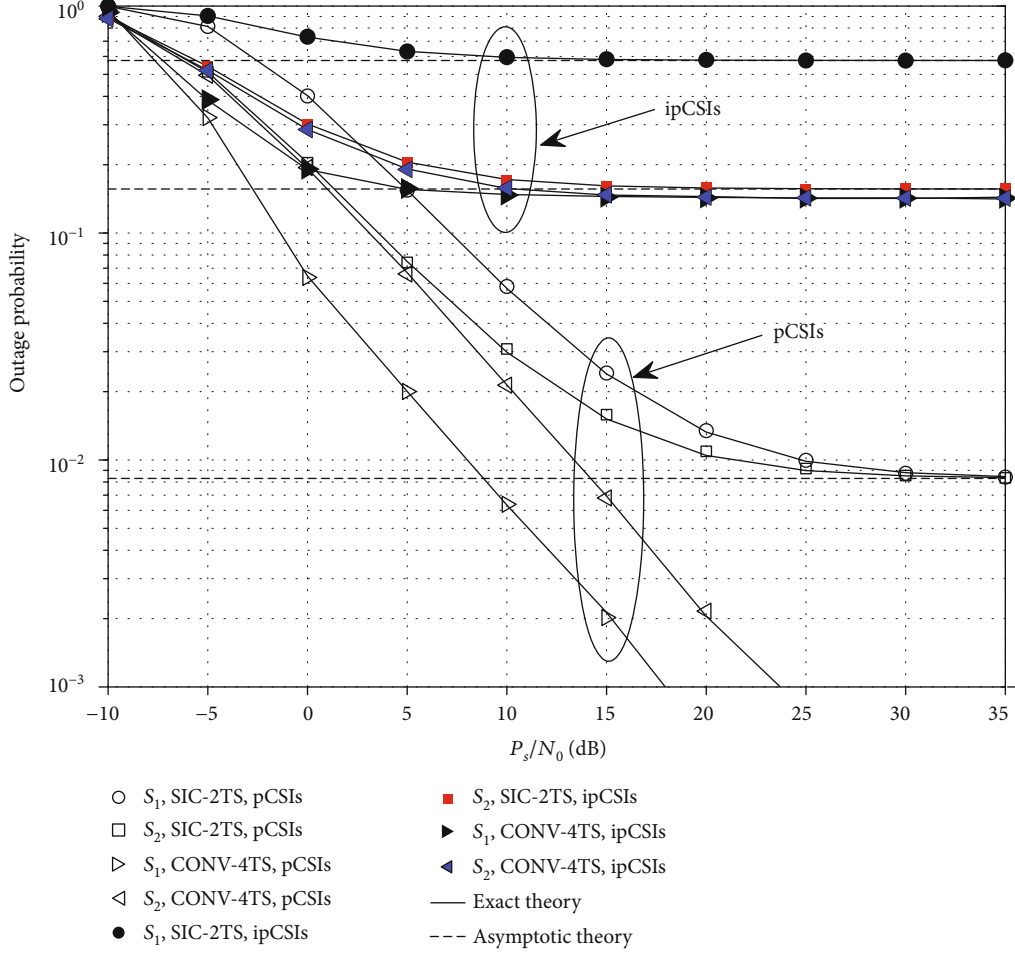


FIGURE 4: Outage probabilities of the source nodes S_1 and S_2 in the proposed SIC-2TS and CONV-4TS protocols versus P_s/N_0 (dB) when $\Omega = -10$ (dB), $d_1 = 0.4$, $d_2 = 1 - d_1$, $N = 6$, pSIC-pCSIs ($\varepsilon = 0$, $\rho = 1$), ipSIC-ipCSIs ($\varepsilon = 1$, $\rho = 0.92$), and the power allocation coefficients $\alpha_1 = \alpha_2 = \eta = 1$.

Corollary 4. When $\gamma \rightarrow +\infty$, we obtain asymptotic expression as

$$\text{OP}_{S_f} \Big|_{d_n \leq d_f}^{\gamma \rightarrow +\infty} = 1 - \left(1 - \lambda_n \sum_{p=0}^N \frac{C_N^p (-1)^p e^{-p\phi_6/\lambda_n}}{\lambda_n + p\phi_2\lambda_f} \right) e^{-\gamma_t(1-\rho^2)}, \quad (24)$$

$$\text{OP}_{S_n} \Big|_{d_n \leq d_f}^{\gamma \rightarrow +\infty} = 1 - \left(\frac{\lambda_f e^{-\phi_7/\lambda_f}}{(\lambda_f + \phi_4\Omega)} - \sum_{p=0}^N \frac{\lambda_n^2 \lambda_f C_N^p (-1)^p e^{-(p(\phi_6 + \phi_7\phi_2)/\lambda_n + \phi_7/\lambda_f)}}{(\lambda_n + p\phi_2\lambda_f)(\lambda_n\lambda_f + \phi_4\Omega(\lambda_n + p\phi_7\phi_2\lambda_f))} \right) e^{-\gamma_t(1-\rho^2)}, \quad (25)$$

where $\phi_6 = (\gamma_t(\alpha_n\lambda_n + \alpha_f\lambda_f)(1-\rho^2))/\alpha_n$ and $\phi_7 = (\gamma_t(\alpha_n\lambda_n + \alpha_f\lambda_f)(1-\rho^2))/\alpha_f$.

Remark 5. In the SIC-3TS protocol, the outage probabilities and the asymptotic expressions of the sources S_f and S_n are

also identified as closed-form formulas (19), (23), (24), and (25), respectively.

4.1.2. The CONV-4TS Protocol. The outage probability at the source S_2 for the $S_1 \xrightarrow[1\text{st}]{x_1} R_{b_1} \xrightarrow[2\text{nd}]{x_1} S_2$ link in the

CONV-4TS protocol is described as follows:

$$\begin{aligned}
\text{OP}_{S_2}^C &= 1 - \Pr \left[\gamma_{S_1 R_{b1}} \geq \gamma_t, \gamma_{R_{b1} S_2} \geq \gamma_t \right] \\
&= 1 - \Pr \left[\gamma_{S_1 R_{b1}} \geq \gamma_t \right] \times \Pr \left[\gamma_{R_{b1} S_2} \geq \gamma_t \right] \\
&= 1 - \left(1 - \Pr \left[\gamma_{S_1 R_{b1}} < \gamma_t \right] \right) \times \left(1 - \Pr \left[\gamma_{R_{b1} S_2} < \gamma_t \right] \right). \tag{26}
\end{aligned}$$

Substituting $\gamma_{S_1 R_{b1}}$ and $\gamma_{R_{b1} S_2}$ in (10) and (12) into ((26), we obtain

$$\begin{aligned}
\text{OP}_{S_2}^C &= 1 - \left(1 - \Pr \left[\frac{\alpha_1 \gamma g_{S_1 R_{b1}}}{\alpha_1 \lambda_1 \gamma (1 - \rho^2) + \rho^2} < \gamma_t \right] \right) \\
&\quad \cdot \left(1 - \Pr \left[\frac{\gamma g_{R_{b1} S_2}}{\gamma \lambda_2 (1 - \rho^2) + \rho^2} < \gamma_t \right] \right) \\
&= 1 - \left(1 - \Pr \left[\underbrace{g_{S_1 R_{b1}} < \gamma_t \lambda_1 (1 - \rho^2) + \gamma_t \rho^2 / (\alpha_1 \gamma)}_{\phi_8} \right] \right) \\
&\quad \times \left(1 - \Pr \left[\underbrace{g_{R_{b1} S_2} < \gamma_t \lambda_2 (1 - \rho^2) + \gamma_t \rho^2 / \gamma}_{\phi_9} \right] \right) \\
&= 1 - \left(1 - F_{g_{S_1 R_{b1}}}(\phi_8) \right) \left(1 - F_{g_{R_{b1} S_2}}(\phi_9) \right) \\
&= 1 - \left(1 - \left(1 - e^{-\phi_8 / \lambda_1} \right)^N \right) e^{-\phi_9 / \lambda_2} \\
&= 1 - \left(1 - \sum_{p=0}^N C_N^p (-1)^p e^{-p \phi_8 / \lambda_1} \right) e^{-\phi_9 / \lambda_2}. \tag{27}
\end{aligned}$$

Similarly, the outage probability at the source S_1 for the $S_2 \xrightarrow[3\text{rd}]{x_2} R_{b2} \xrightarrow[4\text{th}]{x_2} S_1$ link is expressed as

$$\begin{aligned}
\text{OP}_{S_1}^C &= 1 - \Pr \left(\gamma_{S_2 R_{b2}} \geq \gamma_t, \gamma_{R_{b2} S_1} \geq \gamma_t \right) \\
&= 1 - \Pr \left(\gamma_{S_2 R_{b2}} \geq \gamma_t \right) \times \Pr \left(\gamma_{R_{b2} S_1} \geq \gamma_t \right). \tag{28}
\end{aligned}$$

By substituting $\gamma_{S_2 R_{b2}}$ and $\gamma_{R_{b2} S_1}$ in (13) and (14), respectively, into (28) and after some manipulations as finding the outage probability $\text{OP}_{S_2}^C$, we get a final result as

$$\text{OP}_{S_1}^C = 1 - \left(1 - \sum_{p=0}^N C_N^p (-1)^p e^{-p \phi_{10} / \lambda_2} \right) e^{-\phi_{11} / \lambda_1}, \tag{29}$$

$\rho^2) + \gamma_t \rho^2 / \gamma$.

Corollary 6. When $\gamma \rightarrow \infty$, asymptotic expressions of the outage probabilities at the sources S_2 and S_1 are obtained as

$$\begin{aligned}
\text{OP}_{S_2}^C \Big|_{\gamma \rightarrow \infty} &= 1 - \left(1 - \sum_{p=0}^N C_N^p (-1)^p e^{-p \gamma_t (1 - \rho^2)} \right) e^{-\gamma_t (1 - \rho^2)}, \\
\text{OP}_{S_1}^C \Big|_{\gamma \rightarrow \infty} &= 1 - \left(1 - \sum_{p=0}^N C_N^p (-1)^p e^{-p \gamma_t (1 - \rho^2)} \right) e^{-\gamma_t (1 - \rho^2)}. \tag{30}
\end{aligned}$$

4.2. Throughput Analysis. The system throughput of the SIC-2TS, SIC-3TS, and the CONV-4TS protocols is obtained in the following, respectively [39]:

$$\text{TP}_{\text{SIC-2TS}} \Big|_{d_n \leq d_f} = \frac{1}{2} \left(1 - \text{OP}_{S_n} \Big|_{d_n \leq d_f} \right) R_t + \frac{1}{2} \left(1 - \text{OP}_{S_f} \Big|_{d_n \leq d_f} \right) R_t, \tag{31}$$

$$\text{TP}_{\text{SIC-3TS}} \Big|_{d_n \leq d_f} = \frac{1}{3} \left(1 - \text{OP}_{S_n} \Big|_{d_n \leq d_f} \right) R_t + \frac{1}{3} \left(1 - \text{OP}_{S_f} \Big|_{d_n \leq d_f} \right) R_t, \tag{32}$$

$$\text{TP}_{\text{CONV-4TS}} = \frac{1}{4} \left(1 - \text{OP}_{S_1}^C \right) R_t + \frac{1}{4} \left(1 - \text{OP}_{S_2}^C \right) R_t, \tag{33}$$

where 1/2, 1/3, and 1/4 denote that the protocols SIC-2TS, SIC-3TS, and CONV-4TS work in two, three, and four time slots, respectively; $R_t = \log_2(1 + \gamma_t)$ (bits/s/Hz) [40].

Remark 7. The SIC-3TS protocol without the DNC operates in three time slots to send two data; thus, the throughput is obtained by the formula (32) where the outage probabilities $\text{OP}_{S_n} \Big|_{d_n \leq d_f}$ and $\text{OP}_{S_f} \Big|_{d_n \leq d_f}$ are taken from the proposed SIC-2TS protocol.

5. Numerical Results and Discussion

In this section, the outage probabilities and system throughput of three protocols SIC-2TS, SIC-3TS, and CONV-4TS are analyzed and evaluated. The exactness of the asymptotic and exact theory extractions is validated by Monte Carlo simulations (simulated results are shown by the marker point in all figures). We default the threshold SINR as $\gamma_t = 1$ and the path-loss exponent as $\beta = 3$ in all the analyses and evaluations. From Figures 2–5, the distance d_1 has smaller value and $d_2 = 1 - d_1$.

In Figure 2, we examine the outage probabilities of the two sources S_1 and S_2 in the proposed SIC-2TS protocol as a function of the P_S/N_0 (dB) with assuming perfect CSIs ($\rho = 1$) when $\Omega = -10$ (dB), $d_1 = 0.4$, $d_2 = 1 - d_1$, $N \in \{2, 6\}$, and $\alpha_1 = \alpha_2 = \eta = 1$ in both pSIC case ($\varepsilon = 0$) and ipSIC case ($\varepsilon = 1$). Figure 2 shows that the outage probabilities of the source S_2 are equal in the pSIC case and the ipSIC case as formula (19). The outage probabilities of the source S_1 in the pSIC case are higher than those of the source S_2 at the low P_S/N_0 (dB) regions, and they move to the same saturation values at the high P_S/N_0 (dB) regions. The outage

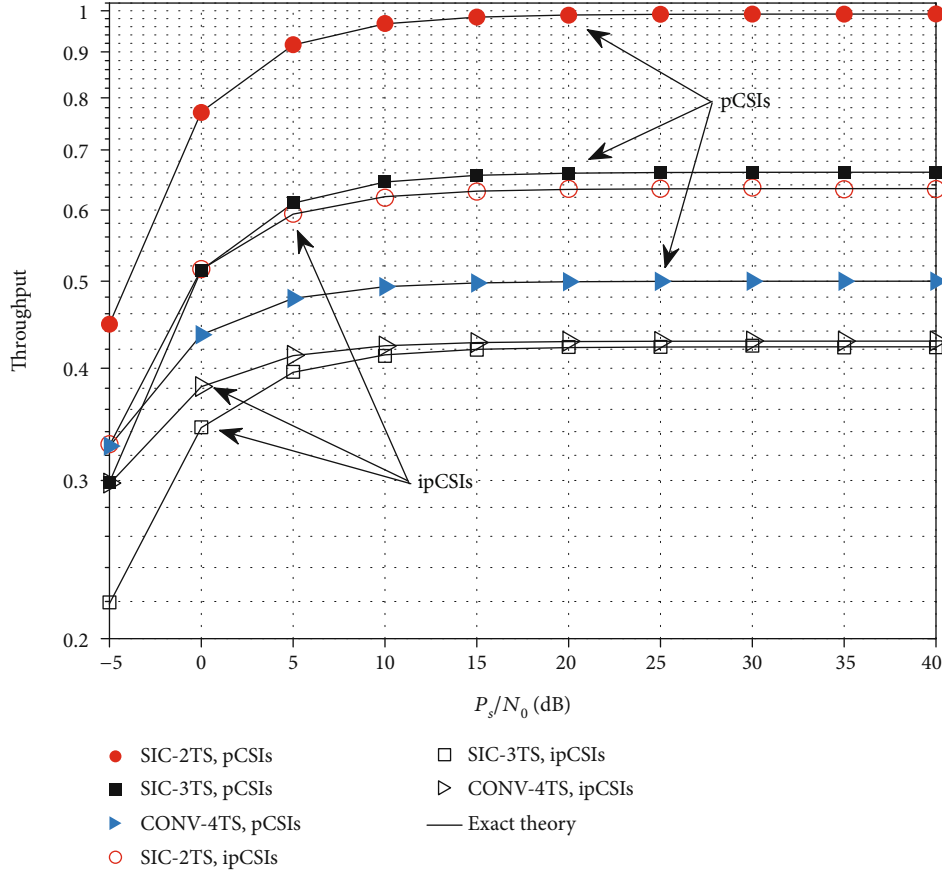


FIGURE 5: Throughput of the SIC-2TS, SIC-3TS, and CONV-4TS protocols versus P_s/N_0 (dB) when $\Omega = -10$ (dB), $d_1 = 0.4$, $d_2 = 1 - d_1$, $N = 6$, $\varepsilon = 0$, $\rho \in \{0.92, 1\}$, and the power allocation coefficients $\alpha_1 = \alpha_2 = \eta = 1$.

probabilities of the source S_1 in the ipSIC case are higher than those in the pSIC case with every P_s/N_0 (dB) due to adding the residual interference signals to the SINR of the signal x_2 at the relay as in formulas (6). Furthermore, the system diversity capacity increases because of using the relay selection methods as in (5) and (17) so the system performance of the proposed SIC-2TS protocol is better when the number of relays increases. Finally, the asymptotic and exact theory analysis lines of the outage probabilities also coincide well with their Monte Carlo simulation lines.

Figure 3 illustrates the outage probabilities of the sources S_1 and S_2 in the proposed SIC-2TS protocol as a function of P_s/N_0 (dB) in both ideal (pSIC-pCSIs) and practical (ipSIC-ipCSIs) conditions when $\Omega = -10$ (dB), $d_1 = 0.4$, $d_2 = 1 - d_1$, $N = 6$, and the power allocation coefficients $\alpha_1 = \alpha_2 = \eta = 1$. Figure 3 shows that the outage probabilities of the two sources with the pSIC- pCSI condition are better than with the ipSIC-ipCSI condition. In the pSIC-pCSI condition, the outage probabilities of the two source nodes have a small difference. But in the ipSIC-ipCSI case, the system outage probability for the source nodes S_1 is a lot higher. These results happen because the SIC technique is used to decode the signal at the relay to make the signal of the farther source more influenced in imperfect cases. In order to have fairness, meaning the two sources can have the nearly same system

outage probability in the ipSIC-ipCSI condition, we can provide the higher transmit power for the farther source by changing the transmit power coefficients (α_1, α_2) in formula (2). Finally, the asymptotic and exact theory analysis lines of the outage probabilities also coincide well with their Monte Carlo simulation lines.

In Figure 4, we consider the outage probabilities of the two sources S_1 and S_2 in the proposed SIC-2TS and CONV-4TS protocols as a function of P_s/N_0 (dB) with assuming perfect SIC ($\varepsilon = 0$) when $\Omega = -10$ (dB), $d_1 = 0.4$, $d_2 = 1 - d_1$, $N = 6$, and $\alpha_1 = \alpha_2 = \eta = 1$ [5, 13] in both pCSI case ($\rho = 1$) and ipCSI case ($\rho = 0.92$). Considering the SIC-2TS protocol in Figure 4, firstly, the outage probabilities of two sources in the pCSI case are smaller than those in the ipCSI case and all of them have the floor values when P_s/N_0 (dB) is large. Secondly, the outage probabilities of the source S_1 has higher than the source S_2 . Thirdly, if the P_s/N_0 (dB) has enough large value the outage probability of the two sources will be equal in the pCSI condition, but the source S_1 outage probabilities are always bigger than the outage probabilities of the source S_2 at all P_s/N_0 (dB) values in the ipCSI condition. Those SIC-2TS protocol results occur because the negative effects of imperfect CSIs lead to channel gain coefficients decrease as formula (1); and in case of $d_1 \leq d_2$, decoding the signal x_2 is decided by the SIC technique

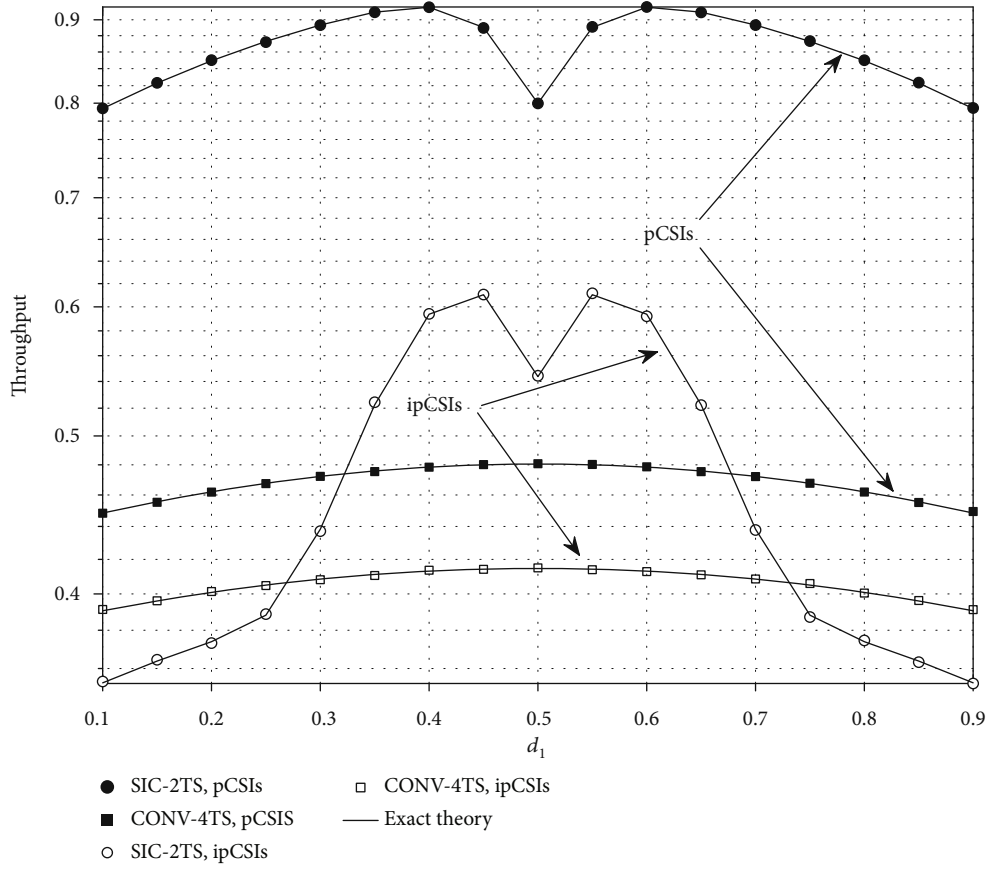


FIGURE 6: Throughput of the SIC-2TS and CONV-4TS protocols versus d_1 when $P_S/N_0 = 5$ (dB), $\Omega = -10$ (dB), $d_2 = 1 - d_1$, $N = 6$, $\varepsilon = 0$, $\rho \in \{0.92, 1\}$, and the power allocation coefficients $\alpha_1 = \alpha_2 = \eta = 1$.

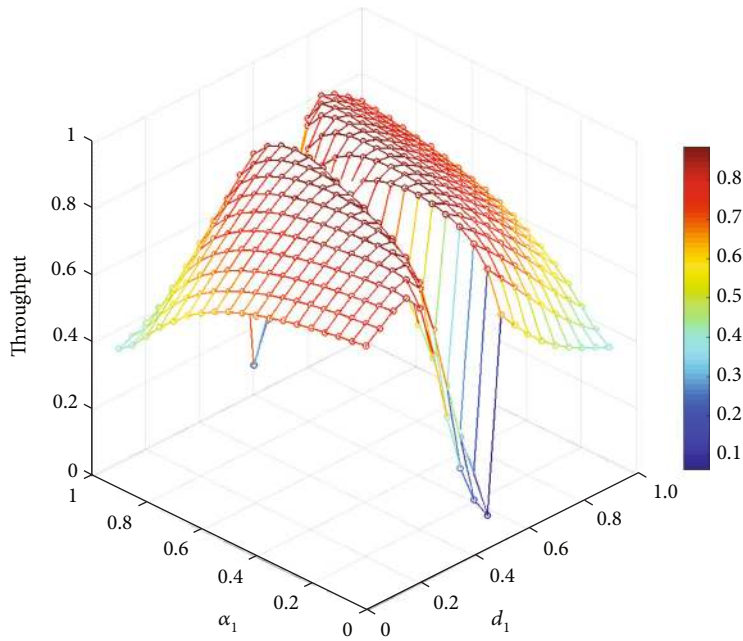
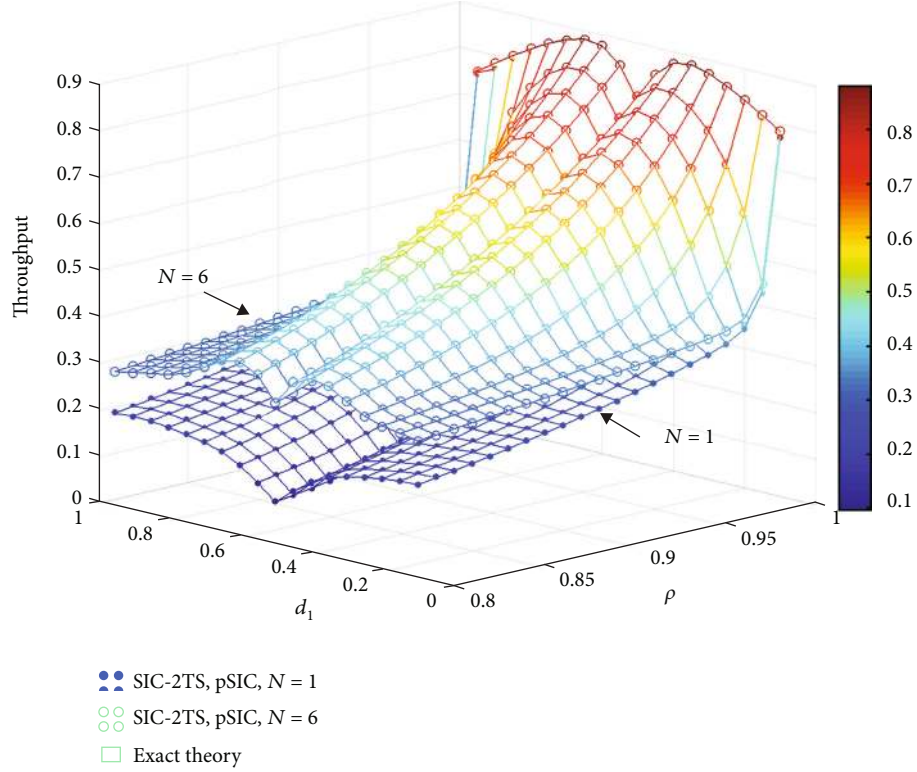


FIGURE 7: Throughput of the SIC-2TS protocol as a function of α_1 and d_1 when $P_S/N_0 = 5$ (dB), $\Omega = -10$ (dB), $d_2 = 1 - d_1$, $N = 6$, $\varepsilon = 0$, $\rho = 1$, and the power allocation coefficients $\alpha_2 = 1 - \alpha_1$ and $\eta = 1$.

TABLE 2: The maximum throughput values corresponding to the distances d_1 and the power allocation coefficient α_1 .

d_1	0.1	0.2	0.3	0.4	0.5	0.6	0.7	0.8	0.9
α_1	0.1	0.1	0.3	0.5	0.3	0.5	0.7	0.9	0.9
Maximum throughput	0.7839	0.8413	0.8715	0.8853	0.8754	0.8853	0.8715	0.8413	0.7839

FIGURE 8: Throughput of the SIC-2TS protocol as a function of d_1 and ρ when $P_S/N_0 = 5(\text{dB})$, $\Omega = -10(\text{dB})$, $d_2 = 1 - d_1$, $N = \{1, 6\}$, $\varepsilon = 0$, $\rho = 0$, $\alpha_1 = d_1$, $\alpha_2 = 1 - \alpha_1$, and $\eta = 1$.

as (4) and (6) so the SINR of the x_2 is affected by the ipCSIs of both links $S_1 \rightarrow R_i$ and $S_2 \rightarrow R_i$. Moreover, we also see that the CONV-4TS protocol has a smaller outage probabilities than the SIC-2TS protocol in both the pCSI and the ipCSI conditions, but this conventional protocol will take a lot of time and energy to transmit the signals. Lastly, the asymptotic and exact theory analysis lines of the outage probabilities coincide well with their Monte Carlo simulation lines.

Figure 5 plots the system throughput for the SIC-2TS, SIC-3TS, and CONV-4TS protocols as a function of P_S/N_0 (dB) with pCSIs/ipCSIs $\rho \in \{0.92, 1\}$ when $\Omega = -10$ (dB), $d_1 = 0.4$, $d_2 = 1 - d_1$, $N = 6$, and the power allocation coefficients $\alpha_1 = \alpha_2 = \eta = 1$ for case $d_1 \leq d_2$ in formulas (31), (32), and (33), respectively. We can see that the proposed SIC-2TS protocol has the ability to achieve higher throughput than the CONV-4TS and SIC-3TS protocols in all P_S/N_0 (dB) for both pCSI and ipCSI cases because it combines the NOMA, SIC, and DNC techniques to help degrade the number of the time slot of the transmission between two sources. In addition, the interference parts on the received SINRs are skipped in the case of pCSIs so the throughput of protocols in this condition is always better than that in the ipCSI condition. Furthermore,

the SIC-2TS protocol throughput converges at the same value in the high P_S/N_0 (dB) regions ($P_S/N_0 > 15$ dB). Finally, the exact theory values of the system throughput of three protocols fix well the Monte Carlo simulations.

Figure 6 demonstrates the system throughput of the SIC-2TS and CONV-4TS protocols versus d_1 in cases of pCSIs/ipCSIs $\rho \in \{0.92, 1\}$ when $P_S/N_0 = 5(\text{dB})$, $\Omega = -10$ (dB), $N = 6$, and the power allocation coefficients $\alpha_1 = \alpha_2 = \eta = 1$. Figure 6 shows that the SIC-2TS protocol has the system throughput higher than the CONV-4TS protocol in the pCSI case. But in the ipCSI case, its throughput is only better when the distances d_1 are about from 0.3 to 0.7. Moreover, the throughput of the SIC-2TS protocol reaches the highest values at optimal locations of the selected relay as $d_1 = 0.4$ (in the pCSIs) and $d_1 = 0.45$ (in the ipCSIs). Besides, the CONV-4TS protocol has the highest system throughput when the relay is at an equidistant point of the two sources ($d_1 = 0.5$). Lastly, in the perfect CSI ($\rho = 1$), the throughput of the two protocols is always better than in the imperfect CSI ($\rho = 0.92$) case.

Figure 7 observes the throughput of the proposed SIC-2TS protocol versus α_1 and d_1 . The scopes of α_1 and d_1 are from 0.05 to 0.95. The throughput of the proposed SIC-2TS protocol

is the highest at about 0.8853 when joint pairs $\{\alpha_1, d_1\} = \{0.4, 0.5\}$ and $\{\alpha_1, d_1\} = \{0.6, 0.5\}$. Table 2 shows the detail of the maximum throughput value corresponding to the distance d_1 and the power coefficient α_1 of the S_1 . The coefficients α_1 and α_2 help to adjust the transmit powers of the source nodes; a smaller power is set to the source node nearer to the relay cluster and higher power for the farther source node. The transmit power allocation can achieve the best throughput performance for the proposed SIC-2TS protocol.

Figure 8 presents the throughput of the proposed SIC-2TS protocol as functions of ρ and d_1 . The range of ρ is from 0.8 to 1, and the range of d_1 is set from 0.05 to 0.95. The power coefficients α_1 and α_2 also vary according to distance d_1 and d_2 , respectively, to achieve the best throughput performance as mentioned in Figure 7. It is seen that a small range decrease in ρ will result in a large range reduction in throughput so obviously, it is necessary to consider the effect of feedback delay when examining a real system. In other words, channel error estimation in cooperation networks becomes principally important and any ineffective estimation can have detrimental consequences for system performance and it should be not omitted when surveying a cooperation network model. Furthermore, the relative distance between the two sources and the relay cluster also affects different throughput decreases as ρ decreases. When the distance d_1 is in the range $[0.3 : 0.4]$ and $[0.6 : 0.7]$, the throughput performance of the system is affected by reduction less than the rest. At last, the larger the number of the relay is, the larger the throughput; therefore, this shows the advantage of using multiple relays.

6. Conclusion

In this article, a two-way cooperative NOMA model with two sources and multiple relaying nodes under the reality conditions as the ip/pCSIs and the ip/pSIC is studied. In the proposed protocol, a relay was selected in the setup phase by the MAC layer protocol to enhance the decoding capacity of the nearer source and minimize the collection time of imperfect CSIs. Spectrum utilization efficiency was improved by using the SIC and DNC techniques at the selected relay. In order to analyze and evaluate the system performance, exact and asymptotic closed-form outage probabilities and throughput expressions were considered and demonstrated by the Monte Carlo simulations. Our results showed that the performance of the proposed SIC-2TS protocol is significantly improved by the increased number of relays as well as the perfect operations of the SIC process and the CSI estimations. Besides, the system performance is decreased in the ipSIC and the ipCSI conditions. The noteworthy thing is found as the proposed SIC-2TS protocol can reach the best performance at optimal locations of the relay cluster and suitable values of power coefficients. In the pCSI condition, the proposed SIC-2TS protocol always has the system performance much better than the CONV-4TS and SIC-3TS protocols. However, in the ipCSI condition, the SIC-2TS protocol only performs better if the distances from two sources to the relay cluster are not very different. Finally, the analysis expressions of the outage probabilities and system throughput are validated by the Monte Carlo simulations.

Appendix

A. Proof of Lemma 2

We have an equivalent expression of $\Pr(\gamma_{S_n R_b \rightarrow x_n | d_n \leq d_f} \geq \gamma_t)$ as

$$\Pr(\gamma_{S_n R_b \rightarrow x_n | d_n \leq d_f} \geq \gamma_t) = 1 - \Pr(\gamma_{S_n R_b \rightarrow x_n | d_n \leq d_f} < \gamma_t). \quad (\text{A.1})$$

Substituting in (4) into (A.1), we have

$$\begin{aligned} & \Pr(\gamma_{S_n R_b \rightarrow x_n | d_n \leq d_f} \geq \gamma_t) \\ &= 1 - \Pr\left(\frac{\alpha_n g_{S_n R_b}}{\alpha_f g_{S_f R_b} + \phi_1} < \gamma_t\right) \\ &= 1 - \Pr\left(g_{S_n R_b} < \underbrace{\frac{\gamma_t \alpha_f}{\alpha_n} g_{S_f R_b}}_{\phi_2} + \underbrace{\frac{\gamma_t \phi_1}{\alpha_n}}_{\phi_3}\right) \\ &= 1 - \Pr(g_{S_n R_b} < \phi_2 g_{S_f R_b} + \phi_3) \\ &= 1 - \int_0^\infty f_{g_{S_f R_b}}(x) F_{g_{S_n R_b}}(\phi_2 x + \phi_3) dx. \end{aligned} \quad (\text{A.2})$$

In (A.2), $F_{g_{S_n R_b}}(x)$ is the CDF of $g_{S_n R_b}$ and can find the following:

$$\begin{aligned} F_{g_{S_n R_b}}(x) &= \Pr[g_{S_n R_b} < x] = \Pr\left[\max_{i=1,2,\dots,N} g_{S_n R_i} < x\right] \\ &= \prod_{i=1}^N \Pr[g_{S_n R_i} < x] \\ &= \prod_{i=1}^N F_{g_{S_n R_i}}(x) = \left(1 - e^{-x/\lambda_n}\right)^N. \end{aligned} \quad (\text{A.3})$$

Substituting the PDF of $g_{S_f R_b}$ as $f_{g_{S_f R_b}}(x) = (1/\lambda_f)e^{-x/\lambda_f}$ and (A.3) into (A.2), we obtain a result as

$$\begin{aligned} & \Pr(\gamma_{S_n R_b \rightarrow x_n | d_n \leq d_f} \geq \gamma_t) \\ &= 1 - \int_0^\infty \frac{1}{\lambda_f} e^{-x/\lambda_f} \left(1 - e^{-(\phi_2 x + \phi_3)/\lambda_n}\right)^N dx \\ &= 1 - \int_0^\infty \frac{1}{\lambda_f} e^{-x/\lambda_f} \sum_{p=0}^N C_N^p (-1)^p e^{-p(\phi_2 x + \phi_3)/\lambda_n} dx \\ &= 1 - \frac{1}{\lambda_f} \sum_{p=0}^N C_N^p (-1)^p e^{-p\phi_3/\lambda_n} \int_0^\infty e^{-x((1/\lambda_f) + (p\phi_2/\lambda_n))} dx \\ &= 1 - \lambda_n \sum_{p=0}^N \frac{C_N^p (-1)^p e^{-p\phi_3/\lambda_n}}{\lambda_n + p\phi_2 \lambda_f}. \end{aligned}$$

Hence, Lemma 2 is proven completely.

B. Proof of Lemma 3

Substituting (4) and (6) into the probability $\Pr(\gamma_{S_n R_b \rightarrow x_n | d_n \leq d_f} \geq \gamma_t, \gamma_{S_f R_b \rightarrow x_f | d_n \leq d_f} \geq \gamma_t)$, we have

$$\begin{aligned}
& \Pr\left(\gamma_{S_n R_b \rightarrow x_n | d_n \leq d_f} \geq \gamma_t, \gamma_{S_f R_b \rightarrow x_f | d_n \leq d_f} \geq \gamma_t\right) \\
&= \Pr\left[\frac{\alpha_n \mathcal{G}_{S_n R_b}}{\alpha_f \mathcal{G}_{S_f R_b} + \phi_1} \geq \gamma_t, \frac{\alpha_f \mathcal{G}_{S_f R_b}}{\varepsilon \rho^2 \mathcal{G}_{R_b} + \phi_1} \geq \gamma_t\right] \\
&= \Pr\left[\underbrace{\mathcal{G}_{S_n R_b} \geq \frac{\gamma_t \alpha_f}{\alpha_n} \mathcal{G}_{S_f R_b}}_{\phi_2} + \underbrace{\frac{\gamma_t \phi_1}{\alpha_n}}_{\phi_3}, \underbrace{\mathcal{G}_{S_f R_b} \geq \frac{\gamma_t \varepsilon \rho^2}{\alpha_f} \mathcal{G}_{R_b}}_{\phi_4} + \underbrace{\frac{\gamma_t \phi_1}{\alpha_f}}_{\phi_5}\right] \\
&= \int_0^\infty f_{g_b}(z) \left(\int_{\phi_4 z + \phi_5}^\infty f_{g_{S_f R_b}}(x) \left(\int_{\phi_2 x + \phi_3}^\infty f_{g_{S_n R_b}}(y) dy \right) dx \right) dz \\
&= \int_0^\infty f_{g_b}(z) \left(\int_{\phi_4 z + \phi_5}^\infty f_{g_{S_f R_b}}(x) \left(1 - F_{g_{S_n R_b}}(\phi_2 x + \phi_3) \right) dx \right) dz.
\end{aligned} \tag{B.1}$$

Substituting PDF of \mathcal{G}_{R_b} , $\mathcal{G}_{S_f R_b}$, and CDF of $\mathcal{G}_{S_n R_b}$ into (B.1), we obtain

$$\begin{aligned}
& \Pr\left(\gamma_{S_n R_b \rightarrow x_n | d_n \leq d_f} \geq \gamma_t, \gamma_{S_f R_b \rightarrow x_f | d_n \leq d_f} \geq \gamma_t\right) \\
&= \int_0^\infty \frac{1}{\Omega} e^{-z/\Omega} \times \left(\int_{\phi_4 z + \phi_5}^\infty \frac{1}{\lambda_f} e^{-x/\lambda_f} \left(1 - \sum_{p=0}^N C_N^p (-1)^p e^{-p(\phi_2 x + \phi_3)/\lambda_n} \right) dx \right) dz \\
&= \frac{\lambda_f e^{-\phi_5/\lambda_f}}{(\lambda_f + \phi_4 \Omega)} - \sum_{p=0}^N \frac{\lambda_n^2 \lambda_f C_N^p (-1)^p e^{-p(\phi_3 + \phi_2 \phi_5)/\lambda_n + \phi_5/\lambda_f}}{(\lambda_n + p\phi_2 \lambda_f)(\lambda_n \lambda_f + \phi_4 \Omega)(\lambda_n + p\phi_5 \phi_2 \lambda_f)}.
\end{aligned} \tag{B.2}$$

Therefore, Lemma 3 is proven completely.

Data Availability

The data used to support the findings of this study are included in the article.

Conflicts of Interest

The authors declare that they have no conflicts of interest.

References

- [1] Z. Ding, Y. Liu, J. Choi et al., "Application of non-orthogonal multiple access in LTE and 5G networks," *IEEE Communications Magazine*, vol. 55, no. 2, pp. 185–191, 2017.
- [2] L. Dai, B. Wang, Y. Yuan, S. Han, I. Chih-Lin, and Z. Wang, "Non-orthogonal multiple access for 5G: solutions, challenges, opportunities, and future research trends," *IEEE Communications Magazine*, vol. 53, no. 9, pp. 74–81, 2015.
- [3] H. Guo, X. Guo, C. Deng, and S. Zhao, "Performance analysis of IQI impaired cooperative NOMA for 5G-enabled Internet of Things," *Wireless Communications and Mobile Computing*, vol. 2020, Article ID 3812826, 12 pages, 2020.
- [4] Z. Yang, Z. Ding, P. Fan, and N. Al-Dhahir, "The impact of power allocation on cooperative non-orthogonal multiple access networks with SWIPT," *IEEE Transactions on Wireless Communications*, vol. 16, pp. 4332–4343, 2017.
- [5] P. N. Son and T. T. Duy, "A new approach for two-way relaying networks: improving performance by successive interference cancellation, digital network coding and opportunistic relay selection," *Wireless Networks*, vol. 26, no. 2, pp. 1315–1329, 2020.
- [6] X. Yue, Y. Liu, S. Kang, A. Nallanathan, and Z. Ding, "Exploiting full/half-duplex user relaying in NOMA systems," *IEEE Transactions on Communications*, vol. 66, pp. 560–575, 2018.
- [7] X. Li, M. Zhao, Y. Liu, L. Li, Z. Ding, and A. Nallanathan, "Secrecy analysis of ambient backscatter NOMA systems under I/Q imbalance," *IEEE Transactions on Vehicular Technology*, vol. 69, pp. 12286–12290, 2020.
- [8] P. Liu, Z. Tao, Z. Lin, E. Erkip, and S. Panwar, "Advances in smart antennas - cooperative wireless communications: a cross-layer approach," *IEEE Wireless Communications*, vol. 13, pp. 84–92, 2006.
- [9] A. Nosratinia, T. E. Hunter, and A. Hedayat, "Cooperative communication in wireless networks," *IEEE Communications Magazine*, vol. 42, pp. 74–80, 2004.
- [10] F. Xing, H. Yin, X. Ji, and V. C. Leung, "Joint relay selection and power allocation for underwater cooperative optical wireless networks," *IEEE Transactions on Wireless Communications*, vol. 19, pp. 251–264, 2019.
- [11] L. Pan, Z. Li, Z. Wang, and F. Zhang, "Joint relay selection and power allocation for the physical layer security of two-way cooperative relaying networks," *Wireless Communications and Mobile Computing*, vol. 2019, Article ID 1839256, 7 pages, 2019.
- [12] V. Ozduran, "Leakage rate-based untrustworthy relay selection with imperfect channel state information: the outage and security trade-off analysis," *IET Communications*, vol. 13, pp. 1902–1915, 2019.
- [13] T. T. Duy and H. Y. Kong, "Exact outage probability of cognitive two-way relaying scheme with opportunistic relay selection under interference constraint," *IET Communications*, vol. 6, pp. 2750–2759, 2012.
- [14] M. J. Taghiyar, S. Muhaidat, J. Liang, and M. Dianati, "Relay selection with imperfect CSI in bidirectional cooperative networks," *IEEE Communications Letters*, vol. 16, pp. 57–59, 2012.
- [15] P. N. Son and H. Y. Kong, "Exact outage probability of two-way decode-and-forward scheme with opportunistic relay selection under physical layer security," *Wireless Personal Communications*, vol. 77, pp. 2889–2917, 2014.
- [16] K. Ho-Van, "Exact outage analysis of underlay cooperative cognitive networks with reactive relay selection under imperfect channel information," *Wireless Personal Communications*, vol. 84, pp. 565–585, 2015.
- [17] P. N. Son and H. Y. Kong, "Exact outage analysis of energy harvesting underlay cooperative cognitive networks," *IEICE Transactions on Communications*, vol. 98, pp. 661–672, 2015.
- [18] T.-P. Huynh, P. N. Son, and M. Voznak, "Exact outage probability of two-way decode-and-forward NOMA scheme with opportunistic relay selection," *KSII Transactions on Internet and Information Systems*, vol. 13, 2019.
- [19] P. N. Son, "Joint impacts of hardware impairments, imperfect CSIs, and interference constraints on underlay cooperative

- cognitive networks with reactive relay selection,” *Telecommunication Systems*, vol. 71, pp. 65–76, 2019.
- [20] V. Ozduran, B. S. B. Yarman, and J. M. Cioffi, “Opportunistic source-pair selection method with imperfect channel state information for multiuser bi-directional relaying networks,” *IET Communications*, vol. 13, pp. 905–917, 2019.
- [21] X. Li, J. Li, Y. Liu, Z. Ding, and A. Nallanathan, “Residual transceiver hardware impairments on cooperative NOMA networks,” *IEEE Transactions on Wireless Communications*, vol. 19, pp. 680–695, 2019.
- [22] Y. Chen, T. Zhang, Y. Liu, and X. Qiao, “Physical layer security in NOMA-enabled cognitive radio networks with outdated channel state information,” *IEEE Access*, vol. 8, pp. 159480–159492, 2020.
- [23] Z. Ding, M. Peng, and H. V. Poor, “Cooperative non-orthogonal multiple access in 5G systems,” *IEEE Communications Letters*, vol. 19, pp. 1462–1465, 2015.
- [24] T.-T. T. Dao, N.-L. Nguyen, H.-N. Nguyen et al., “Exploiting secure performance of full-duplex decode and forward in optimal relay selection networks,” *Elektronika ir Elektrotechnika*, vol. 24, no. 4, 2018.
- [25] M. Zhang, J. Zheng, and Y. He, “Secure transmission scheme for SWIPT-powered full-duplex relay system with multi-antenna based on energy cooperation and cooperative jamming,” *Telecommunication Systems*, vol. 74, pp. 55–66, 2020.
- [26] A. Agarwal and A. K. Jagannatham, “Performance analysis for non-orthogonal multiple access (NOMA)-based two-way relay communication,” *IET Communications*, vol. 13, pp. 363–370, 2018.
- [27] X. Yue, Y. Liu, S. Kang, A. Nallanathan, and Y. Chen, “Modeling and analysis of two-way relay non-orthogonal multiple access systems,” *IEEE Transactions on Communications*, vol. 66, pp. 3784–3796, 2018.
- [28] X. Wang, M. Jia, I. W.-H. Ho, Q. Guo, and F. C. Lau, “Exploiting full-duplex two-way relay cooperative non-orthogonal multiple access,” *IEEE Transactions on Communications*, vol. 67, pp. 2716–2729, 2018.
- [29] X. Tian, Q. Li, X. Li et al., “I/Q imbalance and imperfect SIC on two-way relay NOMA systems,” *Electronics*, vol. 9, pp. 1–16, 2020.
- [30] X. Li, Q. Wang, Y. Liu, T. A. Tsiftsis, Z. Ding, and A. Nallanathan, “UAV-aided multi-way NOMA networks with residual hardware impairments,” *IEEE Wireless Communications Letters*, vol. 9, no. 9, pp. 1538–1542, 2020.
- [31] F. Wei, T. Zhou, T. Xu, and H. Hu, “Modeling and analysis of two-way relay networks: a joint mechanism using NOMA and network coding,” *IEEE Access*, vol. 7, pp. 152679–152689, 2019.
- [32] T.-T. T. Dao and P. N. Son, “Uplink non-orthogonal multiple access protocol in two-way relaying networks: realistic operation and performance analysis,” in *2020 7th NAFOSTED Conference on Information and Computer Science (NICS)*, pp. 399–404, Ho Chi Minh City, Vietnam, 2020.
- [33] Z. Cao, X. Ji, J. Wang, S. Zhang, Y. Ji, and J. Wang, “Security-reliability tradeoff analysis for underlay cognitive two-way relay networks,” *IEEE Transactions on Wireless Communications*, vol. 18, pp. 6030–6042, 2019.
- [34] X. Ding, T. Song, Y. Zou, X. Chen, and L. Hanzo, “Security-reliability tradeoff analysis of artificial noise aided two-way opportunistic relay selection,” *IEEE Transactions on Vehicular Technology*, vol. 66, pp. 3930–3941, 2017.
- [35] H. A. Suraweera, P. J. Smith, and M. Shafi, “Capacity limits and performance analysis of cognitive radio with imperfect channel knowledge,” *IEEE Transactions on Vehicular Technology*, vol. 59, pp. 1811–1822, 2010.
- [36] H. Huang, Z. Li, J. Si, and L. Guan, “Underlay cognitive relay networks with imperfect channel state information and multiple primary receivers,” *IET Communications*, vol. 9, pp. 460–467, 2014.
- [37] H. Cui, R. Zhang, L. Song, and B. Jiao, “Capacity analysis of bidirectional AF relay selection with imperfect channel state information,” *IEEE Wireless Communications Letters*, vol. 2, pp. 255–258, 2013.
- [38] R. Jiang, K. Xiong, P. Fan, L. Zhou, and Z. Zhong, “Outage probability and throughput of multirelay SWIPT-WPCN networks with nonlinear EH model and imperfect CSI,” *IEEE Systems Journal*, vol. 14, pp. 1206–1217, 2020.
- [39] P. N. Son and T. T. Duy, “Performance analysis of underlay cooperative cognitive full-duplex networks with energy-harvesting relay,” *Computer Communications*, vol. 122, pp. 9–19, 2018.
- [40] A. A. Nasir, X. Zhou, S. Durrani, and R. A. Kennedy, “Relaying protocols for wireless energy harvesting and information processing,” *IEEE Transactions on Wireless Communications*, vol. 12, no. 7, pp. 3622–3636, 2013.